Chaotic Modeling and Simulation (CMSIM) 4: 403–414, 2018

The positive influence of Allee effect on synchronization of von Bertalanffy' models

Sandra M. Aleixo[1] and Acilina Caneco[2]

[1] Department of Mathematics, ISEL - Instituto Superior de Engenharia de Lisboa, Instituto Politécnico de Lisboa, Rua Conselheiro Emídio Navarro, 1, 1959-007 Lisboa, Portugal and Centro de Estatística e Aplicações, Faculdade de Ciências, Universidade de Lisboa, 1749-016 Lisboa, Portugal
(E-mail: sandra.aleixo@adm.isel.pt)

[2] Department of Mathematics, ISEL - Instituto Superior de Engenharia de Lisboa, Instituto Politécnico de Lisboa, Rua Conselheiro Emídio Navarro, 1, 1959-007 Lisboa, Portugal and Centro de Investigação em Matemática e Aplicações, Colégio Luís Verney, Rua Romão Ramalho, 59, 7000-671 Évora, Portugal
(E-mail: acilina@adm.isel.pt)

Abstract. The main purpose of this work is to study the relationship between the Allee effect and the synchronization. In general it was believed that, due to competition for resources, a population will have a reduced growth rate at higher densities and increased growth rate at lower densities. However, Warder Clyde Allee introduced the idea that the reverse is true. When the population density is low, the growth rate is reduced and there is a critical population size, the Allee point, below which the population becomes extinct. The extinction of a population is not always a fact to avoid. Indeed, extinguishing a population of cancer cells is an important goal. When the population density is low, individuals require the help of others to survive, and it has been repeatedly reported by some biologists that there is a positive influence of the Allee effect on the cooperation, or synchronism, of populations. Using Bertalanffys models, in which were introduced Allee effect factors, we study the evolution of the synchronizability when the Allee point increases. In fact, our numerical results show that, when the Allee effect gets stronger, the synchronization improves. Considering any fixed network, coupling several nodes having in each one the same dynamical system modeled by Bertalanffy's equation, we observed that the synchronization begin at a lower value of the coupling parameter and the amplitude of the synchronization interval becomes larger. These results confirm the experimental observations of biologists.

Keywords: Synchronization, Allee effect, von Bertalanffy's models, Symbolic dynamics, Chaotic region.

1 Introduction

The Allee effect is an important dynamic phenomenon first described by Allee in 1931, [1]. The generally accepted definition of Allee effect is a correlation

Received: 2 June 2018 / Accepted: 24 October 2018

ISSN 2241-0503

between population size or density and the mean individual performance, often measured as per capita population growth rate of a population or species. Stephens *et al* in 1999, [26], distinguish between component Allee effect (that is a positive relationship between any measurable component of individual performance and population density) and demographic Allee effect (that is a positive relationship between the overall individual performance and population density.

The demographic Allee effect can be classified as either weak or strong. A population exhibiting a weak Allee effect will possess a reduced per capita growth rate (directly related to individual fitness of the population) at lower population density or size. However, even at this low population size or density, the population will always exhibit a positive per capita growth rate. Meanwhile, a population exhibiting a strong Allee effect will have a critical population size or density, the Allee point, under which the population growth rate becomes negative. Therefore, when the population density or size hits a number below this threshold, the population will be extincted. The Allee point is the minimal population size required for growth. The Allee effects should be of great concern to those attempting to assess risk of species extinction. See for example [12] and [19]. On the other hand, the extinction of a cancer tumor cell population will be a good goal that eventually can be achieved by increasing the Allee effect. In fact, increasing growth thresholds and strengthening cooperation reduces the growth of cancer cells and could be an important treatment strategy, [13].

Synchronization is a fundamental nonlinear phenomenon which can be observed in many systems modelling real life [2]. In population dynamics it can be observed on the level of single cells and even on the level of large populations [24] [7] [10]. On the other hand, spatial synchronization can promote global population extinctions [16].

Experimental evidence suggests that for species under a strong Allee effect, the training and group cohesion may be crucial to enhance survival. The animals can reach this collective behaviour through local interactions. Each individual interacts locally with conspecifics and, on the scale of the group, a collective behaviour (synchronization) emerges: animals move together, choose the same patch habitat to live and show a tendency to migrate collectively. That is, a strong Allee effect seems to improve synchronization, [9]. In this work we conduct mathematical analyses, using von Bertalanffy's models, to support this assumption.

The growth of individuals within a population is usually modeled by a function which represents the growth of an "average" individual in the population. The growth of an individual is regarded as an increase in its length or weight with increasing age. Among the various functions or models that have been used to analyze the increase in average length or weight of animals such as fish, marine birds or chick, is the von Bertalanffy's model, one of the most popular, see for example [6], [8] and references therein.

The layout of this work is as follows. In Section 2, we introduce some basic results about network synchronization and we present a process based on symbolic dynamic, in order to find the chaotic region of the generalized von Bertalanffy's models. In Section 3, we describe the von Bertalanffy's models without and with Allee effect and, we determine the chaotic region of this

generalized one. In Section 4, we show some results of our numerical simulations for the Lyapunov exponent, which allow us to relate the synchronizability of the network with the Allee point.

2 Preliminaries

In this section, we present some basic results required for the rest of the paper. First, we introduce some important notions about network synchronization and, in second, we remember some knowledge about symbolic dynamics and topological entropy.

2.1 Network synchronization

Mathematically, networks are described by graphs and the theory of dynamical networks is a combination of graph theory and nonlinear dynamics. From the point of view of dynamical systems, we have a global dynamical system emerging from the interactions between the local dynamics of the individual elements and then, graph theory analyzes the coupling structure.

A graph is a set $G = (V(G), E(G))$ where $V(G)$ is a nonempty set of N vertices or nodes and $E(G)$ is the set of m edges or links e_{ij} that connect two vertices v_i and v_j, [5]. If the graph is weighted, for each pair of vertices (v_i, v_j) we set a non negative weight a_{ij} such that $a_{ij} = 0$ if the vertices v_i and v_j are not connected. If the graph is not weighted, $a_{ij} = 1$ if v_i and v_j are connected and $a_{ij} = 0$ if the vertices v_i and v_j are not connected. If the graph is not directed, $a_{ij} = a_{ji}$. The matrix $A = A(G) = [a_{ij}]$, where v_i, $v_j \in V(G)$, is called the adjacency matrix. The degree of a node v_i is the number of edges incident on it and is represented by k_i, that is, $k_i = \sum_{i=1}^{i=N} a_{ij}$.

Consider the diagonal matrix $D = D(G) = [d_{ij}]$, where $d_{ii} = k_i$. We call Laplacian matrix to $L = D - A$. The eigenvalues of L are all real and non negatives and are contained in the interval $[0, \min\{N, 2\Delta\}]$, where Δ is the maximum degree of the vertices. The spectrum of L may be ordered, $\lambda_1 = 0 \leq \lambda_2 \leq \cdots \leq \lambda_N$. The second eigenvalue λ_2 is know as the algebraic connectivity or Fiedler value and plays a special role in the graph theory. As much larger λ_2 is, more difficult is to separate the graph in disconnected parts. The graph is connected if and only if $\lambda_2 \neq 0$. In fact, the multiplicity of the null eigenvalue λ_1 is equal to the number of connected components of the graph. As we will see later, as bigger is λ_2, more easily the network synchronizes.

Consider a network of N identical chaotic dynamical oscillators, described by a connected, unoriented graph, with no loops and no multiple edges. In each node the dynamics of the oscillators is defined by $\dot{x}_i = f(x_i)$, with $f : \mathbb{R}^n \to \mathbb{R}^n$ and $x_i \in \mathbb{R}^n$ the state variables of the node i.

The state equations of this network are

$$\dot{x}_i = f(x_i) + c\sum_{j=1}^{N} l_{ij}x_j, \qquad \text{with} \quad i = 1, 2, ..., N. \tag{1}$$

where $c > 0$ is the coupling parameter, $A = [a_{ij}]$ is the adjacency matrix and $L = (l_{ij}) = D - A$ is the Laplacian matrix or coupling configuration of the network. The network (1) achieves asymptotical synchronization if $x_1(t) = x_2(t) = ... = x_N(t) \underset{t\to\infty}{\to} e(t)$, where $e(t)$ is a solution of an isolate node (equilibrium point, periodic orbit or chaotic attractor), satisfying $\dot{e}(t) = f(e(t))$.

Consider the network (1) with identical chaotic nodes. The network equations in the discretized form are

$$x_i(k+1) = f(x_i(k)) + c\sum_{j=1}^{N} l_{ij} f(x_j(k)), \qquad \text{with} \quad i = 1, 2, ..., N. \tag{2}$$

Let $0 = \lambda_1 < \lambda_2 \leq ... \leq \lambda_N$ be the eigenvalues of the coupling matrix L and let μ be the Lyapunov exponent of each individual n-dimensional node. If $c > \frac{\mu}{|\lambda_2|}$, then the synchronized states are exponentially stable [14]. So, as bigger is λ_2, more easily (for a lower c) the network synchronizes. We may fix f, the local dynamic in each node and vary the connection topology, L, or fix L and vary f. In this work we fix the network configuration and vary the local dynamical f. We consider on each node the same Bertalanffy function with Allee effect, $f = f_r$, and we study the effect of increasing the Allee point on synchronization.

In a chaotic system it is important to measure the sensitivity with respect to initial conditions. One way to do that is to compute the Lyapunov exponents that measure the average rate at which nearby trajectories diverge from each other. Consider the trajectories x_k and y_k, starting from x_0 and y_0, respectively. If both trajectories are, until time k, always in the same linear region, we can write

$$|x_k - y_k| = e^{\gamma k}|x_0 - y_0|,$$

where $\gamma = \frac{1}{k}\sum_{j=0}^{k-1} \ln|f_r'(x_j)|$.

The Lyapunov exponent of a trajectory x_k is defined by

$$\mu = \lim_{k\to+\infty} \frac{1}{k}\sum_{j=0}^{k-1} \ln|f_r'(x_j)|,$$

whenever it exists. The computation of the Lyapunov exponent μ gives the average rate of divergence (if $\mu > 0$), or convergence (if $\mu < 0$) of the two trajectories from each other, during the time interval $[0, k]$, see for example [11]. In particular, for the von Bertalanffy's functions, the Lyapunov exponents depend on one biological parameter, the intrinsic growth rate r.

If the coupling parameter c belongs to the synchronization interval

$$\left]\frac{1-e^{-\mu}}{\lambda_2}, \frac{1+e^{-\mu}}{\lambda_N}\right[\tag{3}$$

then the synchronized states $x_i(t)$, $(i = 1, ...N)$ are exponentially stable, [14]. Fixing the topology of the network, the eigenvalues of the Laplacian λ_2 and λ_N are fixed, so the synchronization only depends on the Lyapunov exponent of each node, μ, which in turn depends on the two biological parameters: von Bertalanffy's growth rate constant and the asymptotic weight.

2.2 Symbolic dynamics and topological entropy

Symbolic dynamics is a theory composed by a set of results and techniques which have a primordial role in the study of qualitative and quantitative properties of discrete dynamical systems. The topological complexity of a dynamical system is usually measured by its topological entropy. This numerical and topological invariant is associated to the growth rate of the several states of dynamical systems, [15], [17], [18] and [25].

Consider a family of unimodal maps, f_r, depending on a parameter r. For each value of this parameter r, the orbit of the critical point c is given by

$$O_r(c) = \left\{x_k : x_k = f_r^k(c),\ k \in \mathbb{N}_0\right\} \tag{4}$$

defined by an iterative process, where

$$x_k = f_r^k(c) = f_r(x_{k-1}),\ \text{with } k \in \mathbb{N}. \tag{5}$$

In order to study the topological properties of these orbits, we associate to each orbit $O_r(c)$ a sequence of symbols, corresponding to the critical point itinerary, denoted by $S^{(r)} = S_0^{(r)} S_1^{(r)} S_2^{(r)} \dots S_k^{(r)} \dots$, with $k \in \mathbb{N}_0$, where $S_k^{(r)}$ belongs to the alphabet $\mathcal{A} = \{L, C, R\}$, with each symbol defined by

$$S_k^{(r)} = \begin{cases} L \text{ if } f_r^k(c) < c \\ C \text{ if } f_r^k(c) = c \\ R \text{ if } f_r^k(c) > c \end{cases}.$$

Note that, the alphabet $\mathcal{A}$ is an ordered set of symbols, corresponding to the intervals of monotonicity and to the critical point of the map f_r. The real line order induces naturally an order relation in the alphabet $\mathcal{A}$, so $L \prec C \prec R$. The space of all symbolic sequences of the alphabet $\mathcal{A}$ is denoted by $\mathcal{A}^{\mathbb{N}}$.

The expansive maps admit Markov partitions, whose existence is implicit in the works of Bowen and Ruelle. In this study, we consider the existence of Markov partitions, which are characterized by the orbit of the critical point of the map f_r, [25].

Consider the set of points corresponding to the k-periodic orbit or kneading sequence of the critical point

$$S^{(r)} = (C S_1^{(r)} S_2^{(r)} \dots S_{k-1}^{(r)})^{\infty} \in \mathcal{A}^{\mathbb{N}}.$$

This set of points determines the Markov partition of the interval $I = [0, 1]$ in a finite number of subintervals, denoted by $\mathcal{P}_I = \{I_1, I_2, \dots, I_{k-1}\}$. The dynamics of the map f_r is completely characterized by the symbolic sequence $S^{(r)}$ associated to the critical point itinerary.

The map f_r and the Markov partition associated, induce a subshift of finite type whose Markov transition matrix $M = [m_{ij}], (k-1) \times (k-1)$, is defined by

$$m_{ij} = \begin{cases} 1, \text{ if } intI_j \subseteq f_r(intI_i) \\ 0, \text{ otherwise} \end{cases}.$$

Usually, the subshift is denoted by $(\sum_M, \sigma)$, where σ is a shift map in $\sum_{k-1}^{\mathbb{N}}$ defined by $\sigma(S_1 S_2 \ldots) = S_2 S_3 \ldots$, with $\sum_{k-1} = \{1, \ldots k-1\}$ corresponding to the $k-1$ subshifts states.

The topological entropy of the map f_r, in the phase space, is defined in the associated symbolic space as the asymptotic growth rate of the admissible words (finite symbolic sequences) in relation to the length of the words, i.e.,

$$h_{top}(f_r) = \lim_{n\to\infty} \frac{\ln N(n)}{n}$$

where $N(n)$ is the number of admissible words of length n. For a subshift of finite type, unidirectional or bidirectional, described by the Markov transition matrix M, the topological entropy is given by $h_{top}(\sigma) = \ln(\lambda_M)$, where λ_M is the spectral radius of the transition matrix M. For a more detailed approach about subshifts of finite type and the Perron-Frobenius Theorem for Markov transition matrix, see [15], [17], [25] and references therein.

3 Chaotic region of von Bertalanffy's models with Allee effect

We start this section with the description of the usual von Bertalanffy's growth models. As these models do not include Allee effect, phenomenon observed in many populations, bellow are presented generalized models that correct this disadvantage. After this presentation, the chaotic region of the generalized von Bertalanffy's growth models is identified and, the correspondent Lyapunov exponent is estimated in order to study the chaotic synchronization.

3.1 The von Bertalanffy's models: usual and generalized

An usual form of von Bertalanffy's growth function is given by

$$W_t = W_\infty \left(1 - e^{-\frac{K}{3}(t-t_0)}\right)^3, \tag{6}$$

where W_t is the weight at age t, W_∞ is the asymptotic weight, K is von Bertalanffy's growth rate constant and t_0 is the theoretical age the animals would have at weight zero, see [6] and [8]. The growth function given by Eq.(6) is solution of the von Bertalanffy's growth equation, which represent the population growth rate (see dashed line in the Fig.1 (a)) and is given by

$$f(W_t) = \frac{dW_t}{dt} = \frac{K}{3} W_t^{\frac{2}{3}} \left(1 - \left(\frac{W_t}{W_\infty}\right)^{\frac{1}{3}}\right), \tag{7}$$

introduced by von Bertalanffy to model animals weight growth, see [3] and [4]. The *per capita* growth rate, associated to this growth model (see dashed line in the Fig.1 (b)), is given by

$$g(W_t) = \frac{f(W_t)}{W_t} = \frac{K}{3} W_t^{-\frac{1}{3}} \left(1 - \left(\frac{W_t}{W_\infty}\right)^{\frac{1}{3}}\right).$$

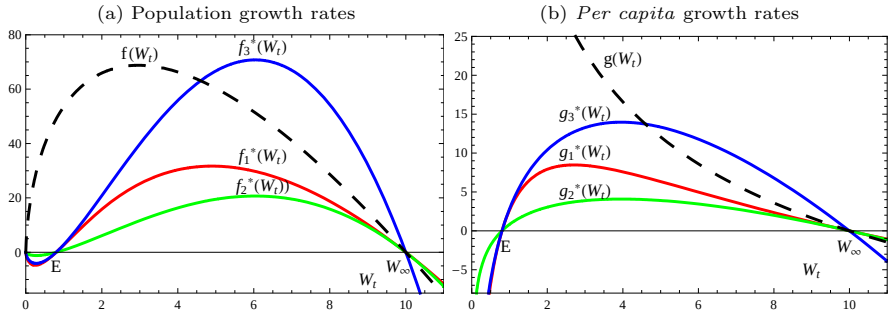

Fig. 1. von Bertalanffy's models without (dashed black line) and with Allee effect (model 1 in red, model 2 in green and model 3 in blue), with $W_\infty = 10$, $C = 3$, $E = 0.8$ and $r = r_i = 100, i = 1, 2, 3$.

However, the von Bertalanffy growth model, Eq.(7), do not exhibit Allee effect, because the *per capita* growth rate decreases at low densities (see dashed line in Fig.1 (b)). Alternative models with Allee effect can be considered using suitable corrections, as was done in [20]. In that paper, it were introduced new correction factors, one of rational type and the others of polynomial type, where two parameters are considered. The use of a parameter $C > 0$ leads to generalization, which yields some more flexible models with variable extinction rates. An Allee point, also called rarefaction critical density or unstable equilibrium, E, is incorporated so that the generalized models have strong Allee effect. The transition from the strong Allee effect to the inexistence of this effect, occurs when a "weakening" of the Allee effect, depending on the parameters C and E, is done.

The corrected or generalized von Bertalanffy growth models, that represent population growth rates (see red, green and blue lines in Fig.1 (a)), were defined in [20] by the differential equations

$$f_i^*(W_t) = \frac{dW_t}{dt} = \frac{K}{3} W_t^{\frac{2}{3}} \left(1 - \left(\frac{W_t}{W_\infty}\right)^{\frac{1}{3}}\right) T_i(W_t), \ i = 1, 2, 3, \qquad (8)$$

where the correction factors which adjust the Allee effect are defined by

$$T_1(W_t) = \frac{W_t - E}{W_t + C}, T_2(W_t) = \frac{W_t - E}{W_\infty + C} \text{ and } T_3(W_t) = \frac{W_t - E}{E + C}$$

with $|E| < W_\infty$ and $C > 0$, where E is the rarefaction critical density or Allee point, W_∞ the carrying capacity, and C is a parameter that allows to define and study more flexible models, with variable extinction rates. The corresponding *per capita* growth rates, associated to these growth models (see red, green and

blue lines in Fig.1 (b)), are given by

$$g_i^*\left(W_t\right) = \frac{f_i^*\left(W_t\right)}{W_t} = \frac{K}{3}\, W_t^{-\frac{1}{3}} \left(1 - \left(\frac{W_t}{W_\infty}\right)^{\frac{1}{3}}\right) T_i\left(W_t\right),\ i = 1, 2, 3.$$

3.2 Chaotic region of the corrected models

To study the chaotic synchronization, we need to identify the chaotic region of these generalized von Bertalanffys models in the parameter space.

We start to consider a family of maps, representing the generalized von Bertalanffy' models with three adjustment factors, which result from the normalization of the population growth rates given by the Eq.(8). These maps $f_{i,r_i} : [0,1] \to]-\infty, 1]$, with $i = 1, 2, 3$, incorporate strong Allee effect and are defined by

$$f_{i,r_i}\left(x\right) = r_i\ x^{\frac{2}{3}} \left(1 - x^{\frac{1}{3}}\right) T_i\left(x\right),\ i = 1, 2, 3 \tag{9}$$

with $x = \frac{W_t}{W_\infty} \in [0,1]$ the normalized weight and $r_i = r_i(K, W_\infty) = \frac{K}{3} \times W_\infty^{\frac{2}{3}} > 0$ $(i = 1, 2, 3)$ an intrinsic growth rate of the individual weight, see an example of model 1 in Fig.2.

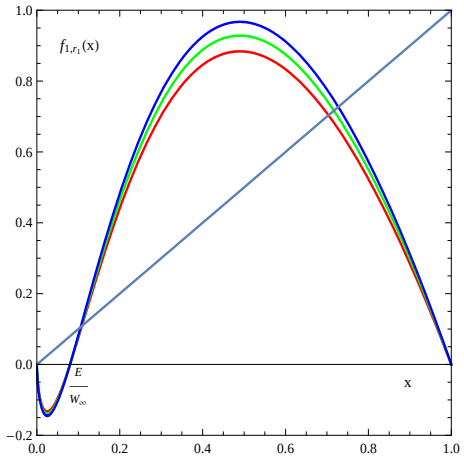

Fig. 2. Graphics of $f_{1;r_1}(x)$, for r_1 (12.95 (red), 13.60 (green) and 14.17 (blue)), with $W_\infty = 10$, $C = 3$ and $E = 0.8$

For each $i = 1, 2, 3$, we consider that $A_{r_i} = f_{i;r_i}\left(A_{r_i}\right)$ is the first positive fixed point of each map $f_{i;r_i}$ and $A_{r_i}^* = max\{f_{i;r_i}^{-1}\left(A_{r_i}\right)\}$. After define these two points A_{r_i} and $A_{r_i}^*$, we consider the following family of unimodal maps $f_{i,r_i} : \left[A_{r_i}, A_{r_i}^*\right] \longrightarrow \left[A_{r_i}, A_{r_i}^*\right]$, which satisfy the following conditions:

- $f_{i;r_i}\left(A_{r_i}\right) = f_{i;r_i}\left(A_{r_i}^*\right) = A_{r_i}$;
- $f_{i;r_i} \in C^3\left(\right]A_{r_i}, A_{r_i}^*\left[\right)$;

- $f'_{i;r_i}(x) \neq 0, \forall x \in \left]A_{r_i}, A^*_{r_i}\right[\setminus \{c_i\}$, ($c_i$ is the positive critical point of each $f_{i;r_i}(x)$);
- $f'_{i;r_i}(c_i) = 0$ and $f''_{i;r_i}(c_i) < 0$;
- the Schwarz derivative of $f_{i;r_i}(x)$ is given by

$$S\left(f_{i;r_i}(x)\right) = \frac{f'''_{i;r_i}(x)}{f'_{i;r_i}(x)} - \frac{3}{2}\left(\frac{f''_{i;r_i}(x)}{f'_{i;r_i}(x)}\right)^2.$$

$S\left(f_{i;r_i}(x)\right) < 0$, for all $x \in \left]A_{r_i}, A^*_{r_i}\right[\setminus \{c_i\}$ and $S\left(f_{i;r_i}(c_i)\right) = -\infty$. This condition ensures a "good" dynamic behaviour of the models: the continuity and monotonicity of topological entropy, the order in the succession of bifurcations, the existence of an upper limit to the number of stable orbits and the non-existence of wandering intervals (Singer's Theorem). In general, the growth models studied have negative Schwarzian derivative and the use of unimodal maps is usual, see for example [21], [22] and [23].

In this work, using the family of unimodal maps defined above, we are only interested in identifying the region of chaos on the parameter space, leaving to another study the detailed analysis of the dynamic behavior of these models. In Fig.3, is represented the bifurcation diagram of the model $f_{1;r_1}$, for some fix values of the parameters, where we can observe, as an example, the dynamic behaviour of the generalized models. The symbolic dynamics techniques prove to be a good methodology to determine by numerical approximation the several regions of the parameter plane, namely the chaotic region. Commonly, the symbolic sequence that identifies the beginning of chaos is $\left(CRLR^3\right)^\infty$, a 6-periodic orbit, see for example [21] and [22]. In the chaotic region of the (K, W_∞) parameter plane, the evolution of the population size is *a priori* unpredictable. The maps are continuous on the interval with positive topological entropy, whence they are chaotic and the Sharkovsky ordering is verified. The symbolic dynamics are characterized by iterates of the functions $f_{i;r_i}$ that originate orbits of several types, which already present chaotic patterns of behavior. The topological entropy is a non-decreasing function in order to the parameter r_i, beeing always less or equal to $\ln 2$ (consequence of the negative Schwartzian derivative). In [21] and [22] can be seen a topological order with several symbolic sequences and their topological entropies, which confirm this result to others growth models. This region is bounded below by the curve of the intrinsic growth rate, r_i, values where the chaos starts. The upper bound it a line designated by chaotic semistability curve, defined by the parameters such that $f^2_{i;r_i}(c_i) = A_{r_i}$, i.e., the maximum size growth is equal to the critical density. This curve characterizes the transition between the chaotic region and an essential extinction region, where the graphic of any function $f_{i;r_i}$ is no longer totally in the invariant set $\left[A_{r_i}, A^*_{r_i}\right]$. For the model 1 exemplified in Fig.3, the chaotic region occurs for values of the intrinsic growth rate, r_1, in the interval $[12.945, 14.177]$.

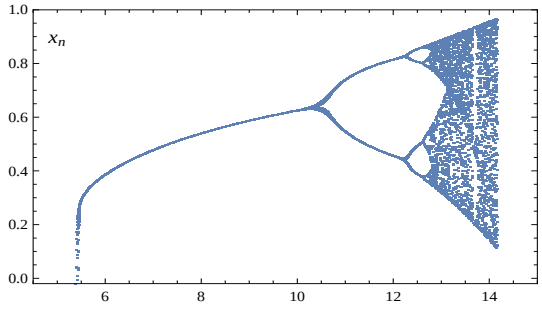

Fig. 3. Bifurcation diagram of $f_{1;r_1}(x)$ for $W_\infty = 10$, $C = 3$ and $E = 0.8$

4 Numerical simulations and conclusions

In this section, we choosed model 1, $f_{1;r_1}$, to make numerical simulations, computing the synchronization interval for several increasing values of E, maintaining fixed the others parameters. We fixed the network, so in the synchronization interval, Eq. (3), the λ_2 and λ_N are fixed. In this case, the network synchronizability depends only on the local dynamic in each node, which is expressed by its Lyapunov exponent μ.

For each value of E, using symbolic dynamics techniques, we obtained the values of the parameter r_1 that bound the chaotic region and then, we selected a range of values of E, for which there is a common range of values of r_1 in the chaotic zone. In this work, we considered three intervals for the Allee point E: $0.1 \leq E \leq 0.5$, $0.6 \leq E \leq 1.0$ and $1.2 \leq E \leq 1.5$, for which we selected the corresponding common chaotic zones $12.16 \leq r_1 \leq 12.34$, $13.54 \leq r_1 \leq 13.60$ and $15.21 \leq r_1 \leq 15.42$, respectively (see Table 1).

E	Chaotic zone lower bound	Chaotic zone upper bound	E	Chaotic zone lower bound	Chaotic zone upper bound	E	Chaotic zone lower bound	Chaotic zone upper bound
0.1	11.17	**12.34**	0.6	12.40	**13.61**	1.1	13.85	15.11
0.2	11.40	12.58	0.7	12.67	13.89	1.2	14.17	**15.44**
0.3	11.64	12.82	0.8	12.95	14.18	1.3	14.50	15.00
0.4	11.88	13.07	0.9	13.24	14.48	1.4	14.85	16.15
0.5	**12.13**	13.34	1.0	**13.53**	14.79	1.5	**15.21**	16.52

Table 1. Intrinsic growth rate, r_1, bounds for the chaotic region, considering model f_{1,r_1}, with several values of the Allee limit E, $W_\infty = 10$, $C = 3$.

For each pair of (E, r_1) values, we numerically compute the Lyapunov exponent using 10000 iterations. The simulation results are presented in Tables 2, 3 and 4.

Fixing the network topology and, as a consequence, fixing λ_2 and λ_N, we can observe that, globally, the Lyapunov exponent decreases as the Allee point increases, when the parameter r is fixed, see Tables 2, 3 and 4. Attending that the synchronization interval is given by Eq. (3), the decrease of the Lyapunov exponent implies: the decreasing of the lower bound and the increase of the upper bound of the synchronization interval. So, as the Allee point E increases,

not only the synchronization begins at a lower value of the coupling parameter c, but also the amplitude of the synchronization interval gets larger. This allow us to conclude that, the synchronization of the network gets better as the Allee point E increases.

$\mathbf{r_1}$	$E = 0.1$	$E = 0.2$	$E = 0.3$	$E = 0.4$	$E = 0.5$
12.16	0.5750	0.4209	0.4188	0.3219	0.1153
12.18	0.5826	0.4500	0.4217	0.3615	0.2333
12.20	0.5790	0.4771	0.4373	0.3698	0.2462
12.22	0.5885	0.4879	0.4374	0.3680	0.2571
12.24	0.6057	0.5003	0.4388	0.3856	0.2752
12.26	0.6214	0.5102	0.4394	0.3789	-0.0954
12.28	0.6280	-0.0527	0.4360	-0.2190	0.3009
12.30	0.6399	0.5013	0.3834	0.3214	0.2654
12.32	0.6558	0.5348	-0.3949	0.3744	0.3316
12.34	0.6778	0.5454	-0.0207	0.3871	0.3468

Table 2. Lyapunov exponent, for μ ($0.1 \leq E \leq 0.5$, $12.16 \leq r_1 \leq 12.34$, $W_\infty = 10$, $C = 3$.

$\mathbf{r_1}$	$E = 0.6$	$E = 0.7$	$E = 0.8$	$E = 0.9$	$E = 1.0$
13.54	0.5923	0.4793	0.4378	0.3583	-0.0780
13.55	0.6266	0.4888	0.4371	0.3677	-0.0561
13.56	0.6320	0.4930	0.4356	0.3672	0.0829
13.57	0.6401	0.5124	0.4226	0.3688	0.2045
13.58	0.6438	0.5112	0.4415	0.3631	0.2286
13.59	0.6531	0.5122	0.4302	0.3745	0.2174
13.60	0.6707	0.4810	0.4354	0.3740	0.2440

Table 3. Lyapunov exponent μ for $0.6 \leq E \leq 1.0$, $13.54 \leq r_1 \leq 13.60$, $W_\infty = 10$, $C = 3$.

$\mathbf{r_1}$	$E = 1.2$	$E = 1.3$	$E = 1.4$	$E = 1.5$
15.21	0.5128	0.4423	0.3682	-0.1583
15.24	0.5309	0.3871	0.3834	0.1875
15.27	0.5573	-0.1978	0.3733	0.2439
15.30	0.5785	-0.0837	0.0867	0.2600
15.33	0.5841	0.2028	0.3684	0.2806
15.36	0.5941	0.4312	0.3872	0.2866
15.39	0.6245	0.4605	0.4077	0.3079
15.42	0.6379	0.4822	0.3971	0.3445

Table 4. Lyapunov exponent μ for $0.6 \leq E \leq 1.0$, $13.54 \leq r_1 \leq 13.60$, $W_\infty = 10$, $C = 3$.

Acknowledgements Research partially funded by ISEL and FCT – Fundação para a Ciência e Tecnologia, Portugal through the projects: UID/MAT/00006/2013, CEAUL and UID/MAT/04674/2013, CIMA-UE.

References

1. W. C. Allee. *Animal aggregations, a study in general sociology*, University of Chicago Press, Chicago, 1931.
2. A. Balanov, N. Janson, D. Postnov and O. Sosnovtseva. *Synchronization: From Simple to Complex*, Springer Series in Synergetics, 2009.
3. L. Bertalanffy. *A quantitative theory of organic growth (inquiries on growth laws II). Human Biology* , 10, 181–213, 1938.
4. L. Bertalanffy. Quantitative laws in metabolism and growth. *The Quarterly Review of Biology*, 32, 217–31, 1957.
5. B. Bollobás. *Random Graphs,*. Academic Press, London, 1985.
6. G. M. Cailliet, W. D. Smith, H. F. Mollet and K. J. Goldman. Age and growth studies of chondrichthyan shes: the need for consistency in terminology, verication, validation and growth function tting. *Environ. Biol. Fish.*, 77, 211–228, 2006.

7. A. Caneco, J. L. Rocha and C. Grácio. Topological Entropy in the Synchronization of Piecewise Linear and Monotone Maps: Coupled Duffing Oscillators. *Int. J. Bifurcation and Chaos*, 19, **11**, 3855–3868, 2009.
8. T. E. Essington, J. F. Kitchell and C. J. Walters. The von Bertalanffy growth function, bioenergetics, and the consumption rates of fish. *Can. J. Fish. Aquat. Sci.*, 58, 2129–2138, 2001.
9. A. A. Fernande. *Influence of the Allee effect and collective behaviour on population dynamics. The case of the two-spotted spider mite*, Dissertation, Universit Libre de Bruxelles, 2011.
10. D. Fournier-Prunaret, J. L. Rocha, A. Caneco, S. Fernandes and C. Grácio. Synchronization and Basins of Synchronized States in Two-Dimensional Piecewise Maps via Coupling Three Pieces of One-Dimensional Maps. *Int. J. Bifurcation and Chaos*, 23, **8**, 1350134, 1–18, 2013.
11. M. Hasler, Y. L. Maistrenko. An Introduction to the Synchronization of Chaotic Systems: Coupled Skew Tent Maps. *IEEE Transactions on Circuits and Systems - I: Fundamental Theory and Applications*, 4, **10**, 856–866, 1987.
12. J. A. Hutchings and J. D. Reynolds. Marine fish population collapses: consequences for recovery and extinction risk. *BioSci*, 54, 297–309, 2004.
13. K. S. Korolev, J. B. Xavier and J. Gore. Turning ecology and evolution against cancer. *Nature Reviews Cancer*, 14, 371–380, 2014.
14. X. Li and G. Chen. Synchronization and desynchronization of complex dynamical networks: An engineering viewpoint. *IEEE Trans. on Circ. Syst. – I*, 50, **11**, 1381–1390, 2003.
15. D. Lind and B. Marcus. *An Introduction to Symbolic Dynamics and Codings*, Cambridge University Press, Cambridge, 1995.
16. V. Manica and J. A. L. Silva. Population distribution and synchronized dynamics in a metapopulation model in two geographic scales. *Mathematical Biosciences* 250, 1–9, 2014.
17. W. Melo and S. van Strien. *One-Dimensional Dynamics*, Springer, New York, 1993.
18. J. Milnor and W. Thurston. On iterated maps of the interval. *Lect. Notes in Math, Springer-Verlag*, 1342, 465–563, 1988.
19. J. A . Musick. Criteria to Define Extinction Risk in Marine Fishes: The American Fisheries Society Initiative. *Fisheries*, 24, 6–14, 1999.
20. J. L. Rocha and S. M. Aleixo. Von Bertalanffy' Growth Dynamics with Strong Allee Effect. *Discussiones Mathematicae. Probability and Statistics*, 32, 35–45, 2013.
21. J. L. Rocha and S. M. Aleixo. An Extension of Gompertzian Growth Dynamics: Weibull and Fréchet Models. *Math. Biosci. Eng.*, 10, 379–398, 2013.
22. J. L. Rocha and S. M. Aleixo. Dynamical Analysis in Growth Models: Blumberg's Equation. *Discrete Contin. Dyn. Syst.- Ser.B*, 18, 783–795, 2013.
23. J. L. Rocha, S. M. Aleixo and Caneco. Synchronization in von Bertalanffy's models. *CMSIM - Chaotic Modeling and Simulation Journal*, 4, 519–528, 2013.
24. J. L. Rocha, S. M. Aleixo and A. Caneco. Synchronization in Richards Chaotic Systems. *Journal of Applied Nonlinear Dynamics*, 3, **2**, 115–130, 2014.
25. J. L. Rocha and J. S. Ramos. Weighted kneading theory of one-dimensional maps with a hole. *Int. J. Math. Math. Sci.*, 38, 2019–2038, 2004.
26. P. A. Stephens, W. J. Sutherland and R. P. Freckleton. What is the Allee effect? *Oikos*, 87, **1**, 185–190, 1999.